SIMULATION OF THE BEHAVIOUR OF THIN-WALLED BEAM-COLUMN WITH NON-SYMMETRICAL CROSS SECTION

Abdel Aziz M. Ibrahim *, Ahmed R. Abo-Tabikh* and Ahmed M. Nour El-Dien **

* Structural Engineering Department, Faculty of Engineering, Alexandria. University
** Arab Construction Group, Alexandria.

ABSTRACT

In this paper, the interaction between local and overall buckling of thin-walled columns under different loading is analyzed by means of the general elastic stability theory. Initial imperfections of the structure and the residual stresses are taken into consideration, a numerical solution is suggested in order to determine the behavior of columns during loading. The validity of the analytical method is verified by comparing its results with previous experimental work. The results of many shapes of cross section under different cases of loading are studied.

Keywords: Thin-walled, Local buckling, Code, Warping deformation, Finite difference.

INTRODUCTION

Local and overall buckling of elastic thin-walled columns are extensively investigated. With the existing number of studies, it was found that most of authors treated this problem by reducing column-flexural stiffness. The results of this method are in good agreement with the experimental results for symmetrical case of loading. The reduction of the column stiffness is generally obtained by applying the formula proposed by G. Winter [1] which is based on the Von Karman [2] formula. These formulas are introduced in almost all design Codes ; for example, the Egyptian Code [3] and AISI [4].

The aim of this study is to present an analytical model which simulate the behavior of a thin-walled beam-column of non symmetrical cross section under unsymmetrical cases of loading, taking into consideration the flexural/flexural-torsional buckling interaction. Effective ones replace the locally buckled column plate-elements. This will also be considered under various stress gradients.

Verification through different experimental works is made and the ultimate loads are compared with Egyptian code [3] and AISI [4]. Results of many shapes of cross-section under different cases of loading are performed.

THEORETICAL MODEL

Assumptions

Considering a thin-walled element as in Figure 1, the following assumptions are adopted:

- Elements are prismatic members.
- Elements are subjected to initial imperfections (deflections and twist).
- Invariability of the cross section until reaching ultimate Limit State.
- Thin-walled open cross section is longitudinally subjected to only normal stresses; shear stresses caused by twisting are following the contour direction of the cross section.
- Shear deformations are ignored so that warping deformation of the cross section can be calculated by the rule of sectorial area.
- Beam-Columns have variable cross section properties depending on the acting stresses (effective cross section).

- The effective cross section is only used for the elastic zone.
- displacements are assumed to be small.

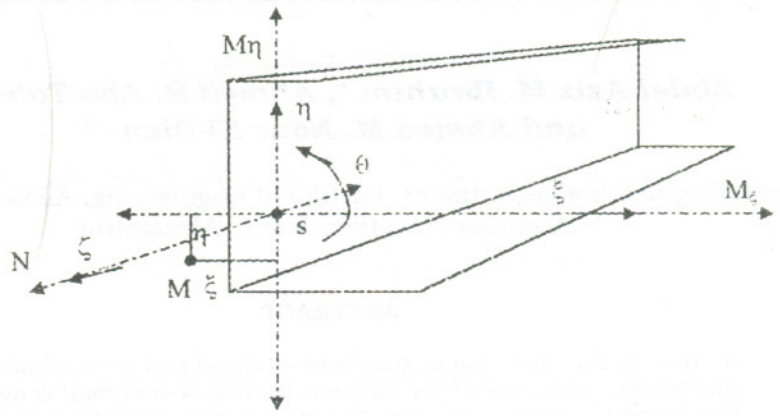

Figure 1 Thin-Walled cross section

GENERALIZED STRESS-STRAIN RELATIONSHIP

For the arbitrary coordinates ξ, η and ω on the cross section, the normal strain ε is related to the generalized strain [5] (axial strain ε_o, biaxial curvatures Φ_ξ and Φ_η and warping curvature θ_ζ') by [5]:

$$\varepsilon=\varepsilon_o+\eta\Phi_\xi-\xi\Phi_\eta-\omega\theta_\zeta'=\varepsilon_o+\eta\theta_\xi'-\xi\theta_\eta'-\omega\theta_\zeta' \qquad (1)$$

in which θ_ξ, θ_η and θ_ζ are rotation angles of the cross section about the coordinate axes ξ, η and ζ respectively. These are related to the curvatures and axial displacement by:

$$\theta_\xi'=\Phi_\xi=-v'' \quad , \quad \theta_\eta'=\Phi_\eta=u'' \text{ and } w=\varepsilon_o \qquad (2)$$

Using Equations 1 and 2, Equation 1 may be rewritten as:

$$\varepsilon=\varepsilon_o-v''\eta-u''\xi-\omega\theta_\zeta' \qquad (3)$$

Since the stress-strain relation is $\sigma=E\varepsilon$, the generalized stress-strain relationship can be presented as:

$$\sigma=E[\varepsilon_o-v''\eta-u''\xi-\omega\theta_\zeta'] \qquad (4)$$

from which the general form of the equilibrium equations[5] is presented as:

$$E\begin{bmatrix} A & S_y & -S_x & -S_\omega \\ S_y & I_x & -I_{xy} & -I_{\omega y} \\ -S_x & -I_{xy} & I_y & -I_{\omega x} \\ S_\omega & I_{\omega} & -I_{\omega x} & -I_\omega \end{bmatrix}\begin{bmatrix} \omega'+0.5(u')^2+0.5(v')^2 \\ -v''+\theta u''-u'\theta' \\ u''+\theta v''-v'\theta' \\ \theta''-u'v''+v'u'' \end{bmatrix} \qquad (5)$$

$$=\begin{bmatrix} 1 & 0 & 0 & 0 & 0 \\ 0 & 1 & \theta & -u' & 0 \\ 0 & -\theta & 1 & -v' & 0 \\ 0 & 0 & 0 & 0 & 1 \end{bmatrix}\begin{bmatrix} F_{zo} \\ M_x-vF_{zo} \\ M_y+uF_{zo} \\ M_{zo}+vF_{xo}-uF_{yo} \\ M_\omega \end{bmatrix}$$

and

$$(-E\,I_\omega\,G\,K_T+\overline{K})\begin{bmatrix} \theta'''-u''v'''+ \\ - \end{bmatrix}$$

$$=(u' \quad v' \quad 1)\begin{bmatrix} M_x-v+\eta_o)F_{zo} \\ M_y+(u+\xi_o)F_{zo} \\ M_{zo}+(v+\eta_o)F_{xo}-(u+\xi_o)F_{yo} \end{bmatrix}$$

Since these differential equilibrium equations are highly nonlinear, some simplifying assumptions must be adopted before an actual solution procedure is attempted. To simphify equation 5, neglect the higher order terms containing the product of derivatives of displacements, then take the principal axes for the cross section coordinates (ξ,η) and the shear center $S(\xi_o,\eta_o)$ as the pole of the normalized warping (see figure 2). Equation of equilibrium Equation 5, becomes:

$$E\begin{bmatrix} A & S_y & -S_x \\ S_y & I_x & -I_{xy} \\ -S_x & I_{xy} & I_y \end{bmatrix}\begin{bmatrix} \omega' \\ -V'' + \theta'' \\ u'' + \theta v'' \end{bmatrix}$$

$$= \begin{bmatrix} 1 & 0 & 0 & 0 \\ 0 & 1 & \theta & -u' \\ 0 & -\theta & 1 & -v' \end{bmatrix}\begin{bmatrix} F_{zo} \\ M_x - vF_{zo} \\ M_y + uF_{zo} \\ M_{zo} + vF_{xo} - uF_{yo} \end{bmatrix} \quad (6)$$

Rewrite equation 6 using the following relations:

$$\begin{aligned} F_{xo} &= M_y' \\ F_{yo} &= M_x \\ F_{zo} &= -P \quad , \quad w' = \varepsilon_o \\ S_x &= S_y = S_\omega = I_{xy} = I_{\omega x} = I_{\omega y} = 0 \end{aligned} \quad (7)$$

Then equation 6 is reduced to :

$$\begin{aligned} &-EA\varepsilon_o = P \\ &-EI_x v'' - EI_x \theta u'' = M_x + [v - \theta u]P + \theta M_y - u'(M_{zo} - vM_y' - uM_x') \\ &EI_y u'' - EI_y \theta v'' = M_y - [u + \theta v]P - \theta M_x - v'(M_{zo} - vM_y' - uM_x') \end{aligned} \quad (8)$$

$$-EI_\omega \theta''' + (GK_T + K)\theta' = u'[M_x + (v+\eta_o)P] + v'[M_y - (u+\xi_o)P] + M_{zo} - (v+\eta_o)M_y' - (u+\xi_o)M_x'$$

In the case of elastic section, the shear center $S(\xi o,\eta o)$ can be clearly defined further. The rotation of the section θ takes place with respect to the shear center; thus Equation 8 can be rewritten in terms of displacements of the shear center:

$$u_m = u - \theta\eta_o \quad \text{and} \quad v_m = v + \theta\xi_o \quad (9)$$

Further, if we neglect all the nonlinear terms of displacements, and Differentiating the first two equations twice and the third one once , the following equations are obtained:

$$\begin{aligned} &EI_x v_m'''' + P(v_m'' - \xi_o\theta'') + M_x'' + M_y\theta'' + M_y''\theta + 2\theta' M_y' \\ &\qquad - u_m''' M_{zo} - 2u_m'' M_{zo}' - u_m' M_{zo}'' = 0 \\ &EI_y u_m'''' + P(u_m'' + \eta_o\theta'') - M_y'' + M_x\theta'' + M_x''\theta + 2\theta' M_x' \\ &\qquad - v_m''' M_{zo} - 2v_m'' M_{zo}' - v_m' M_{zo}'' = 0 \\ &EI_\omega \theta'''' - (GK_T + K)\theta'' - K'\theta' + P(\eta_o u_m'' - \xi_o v_m'') + M_x u_m'' + M_x' u_m' \\ &+ M_y v_m'' + M_y' v_m' + M_{zo}' - (v_m - \theta\xi_o + \eta_o)M_y'' - (u_m + \theta\eta_o + \xi_o)M_x'' \\ &- (v_m' - \theta'\xi_o)M_y' - (u_m' + \theta'\eta_o)M_x' = 0 \end{aligned} \quad (10)$$

These are the basic equations of elastic beam-columns. If the moments are equally at both ends, then:

$$\begin{aligned} M_x &= -P\,ey - Q_y[z - L]z/2 \\ M_y &= P\,ex + Q_x[z - L]z/2 \\ M_x' &= -Q_y[2z - L]/2 \\ M_y' &= Q_x[2z - L]/2 \\ M_x'' &= -Q_y \\ M_y'' &= Q_x \\ M_{zo}' &= M_{zo}'' = 0 \end{aligned} \quad (11)$$

where Q_x, Q_y are The lateral distributed loads acting on the beam-column . Thus, equation 10 can be rewritten as following:

$$\begin{aligned} &EI_x v_m'''' + P\,v_m'' + [P(ex - \xi_o) + Q_x(z - L)z/2]\theta'' + Q_x[2z - L]\theta' + Q_x\theta = Q_y \\ &EI_y u_m'''' + P\,u_m'' - [P(ey - \eta_o) + Q_y[z - L]z/2]\theta'' - Q_y[2z - L]\theta' - Q_y\theta = Q_x \end{aligned} \quad (12)$$

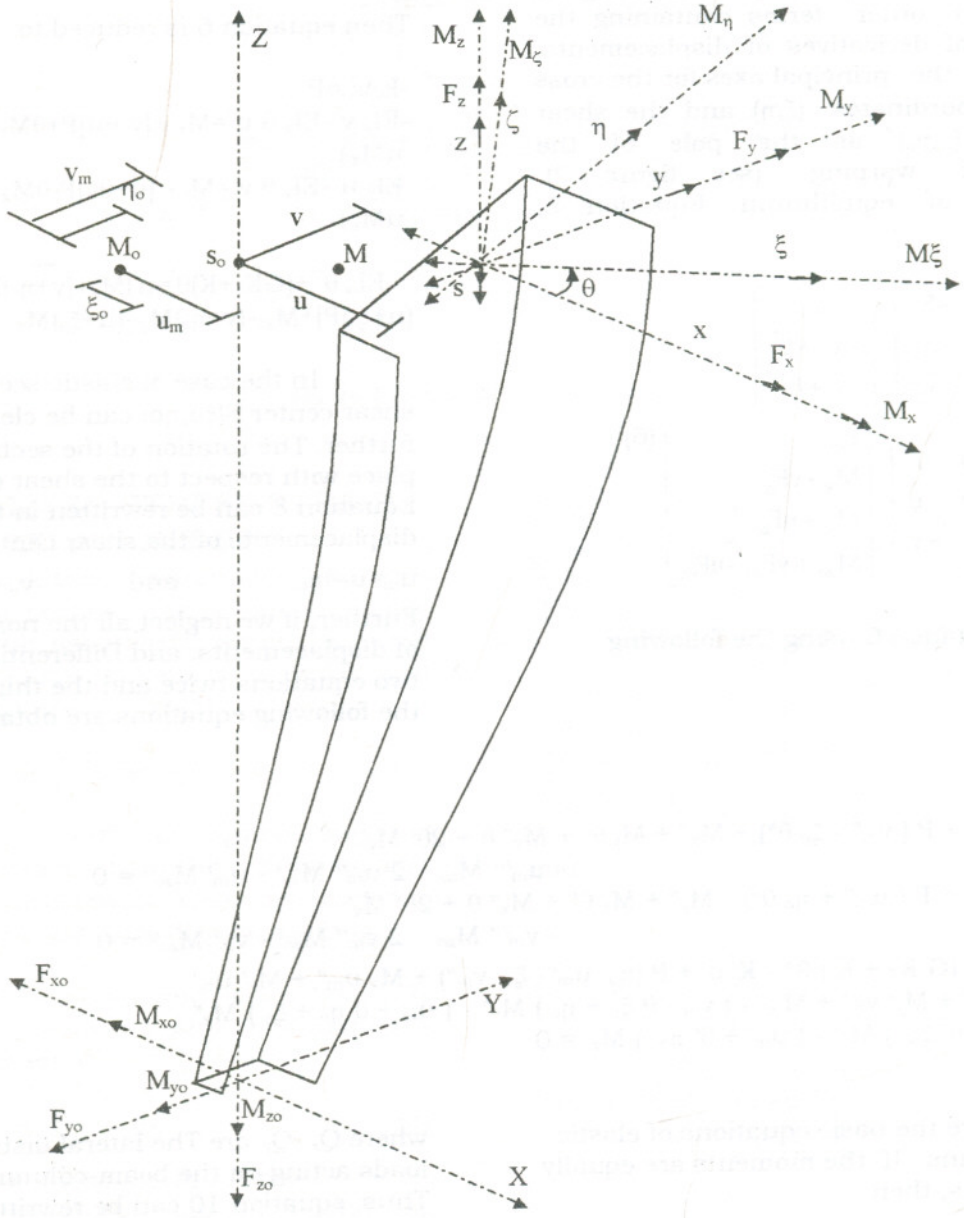

Figure 2 Local and Global axes

- $(G K_T + \overline{K}) \theta'' - \overline{K}' \theta' + (Q_x \xi_o + Q_y$
$- L] / 2 \theta' + (Q_x \xi_o + Q_y \eta_o) \theta + (P (e_x$
$Q_x [z - L] z / 2) v_m'' - (P (e_y - \eta_o) + Q_y [$
$z / 2) u_m'' - Q_x v_m + Q_y u_m = Q_x \eta_o -$

nto consideration the following initial
tions:
l deflection and twist u_o , v_o and θ_o , where:

$$u_o = B_o \sin (\pi z / L)$$
$$v_o = C_o \sin (\pi z / L) \quad (13)$$
$$\theta_o = D_o \sin (\pi z / L)$$

- Effect of a given distribution of a residual stress .
- Effect of local buckling . Three new functions are Introduced such as u_L , v_L , θ_L which represent the displacement of the center of gravity in x and y directions and the rotation of the principal axes respectively , so the differential equations are finally expressed by the form :

$$EI_x v_m'''' + P v_m'' + [P(e_x - \xi_o) + Q_x (z - L) z / 2] \theta'' + Q_x [2z - L] \theta' + Q_x \theta = Q_y + P [C_o (z^2/L^2) \sin (\pi z/L) - vL''] + [P(e_x - \xi_o) + Q_x (z - L) z / 2] [D_o (z^2/L^2) \sin (\pi z/L) - \theta L''] - Q_x [2z - L] [D_o (z/L) \cos (\pi z/L) + \theta L'] - Q_x [D_o \sin (\pi z/L) + \theta L]$$

$$EI_y u_m'''' + P u_m'' - [P(e_y - \eta_o) + Q_y (z - L) z / 2] \theta'' - Q_y [2z - L] \theta' - Q_y \theta = Q_x + P [B_o (z^2/L^2) \sin (\pi z/L) - uL''] - [P(e_y - \eta_o) + Q_y (z - L) z / 2] [D_o (z^2/L^2) \sin (\pi z/L) - \theta L''] + Q_y [2z - L] [D_o (z/L) \cos (\pi z/L) + \theta L'] + Q_y [D_o \sin (\pi z/L) + \theta L] \quad (14)$$

$$EI_\omega \theta'''' - (G K_T + K + \overline{B}) \overline{\theta''} + \{(Q_x \xi_o + Q_y \eta_o)[2z - L] / 2 - K' \} \theta' + (Q_x \xi_o + Q_y \eta_o) \theta + (P (e_x - \xi_o) + Q_x [z - L] z / 2) v_m'' - (P (e_y - \eta_o) + Q_y [z - L] z / 2) u_m'' -$$

$$Q_x v_m + Q_y u_m = Q_x \eta_o - Q_y \xi_o + K [\theta L'' - D_o (z^2/L^2) \sin (\pi z/L)] - \{(Q_x \xi_o + Q_y \eta_o)[2z - L] / 2 \} [D_o (z/L) \cos (\pi z/L) + \theta L'] - (Q_x \xi_o + Q_y \eta_o) [D_o \sin (\pi z/L) + \theta L] + (P (e_x - \xi_o) + Q_x [z - L] z / 2) [C_o (z^2/L^2) \sin (\pi z/L) - vL''] - (P (e_y - \eta_o) + Q_y [z - L] z / 2) [B_o (z^2/L^2) \sin (\pi z/L) - uL''] + Q_x [C_o \sin (\pi z/L) + vL] - Q_y [B_o \sin (\pi z/L) + uL]$$

$= \int \sigma_r (x^2 + y^2) dA$

term $\overline{B}$ in Equation 14 represents ıtribution of the residual stresses to ernal twist moment. Equations 14 are ɛm of three linear inhomogeneous tial equations with three unknowns θ.

NUMERICAL TREATMENT

finite difference method for the of The differential equations is a ıe for the reduction of a continuum ystem with finite number of degrees of . The basic concept of the method is e derivatives of functions at a point e approximated by an algebraic ion consisting of the value of the ı at that point and at several nearly Soltis [6] has extensively discussed this method. The derivations of a function u could be expressed by these forms:

$$u_i' = \frac{1}{2\Delta z} (u_{i+1} - u_{i-1}) \quad (15)$$

$$u_i'' = \frac{1}{(\Delta z)^2} (u_{i+1} - 2u_i + u_{i-1}) \quad (16)$$

$$u_i''' = \frac{1}{2(\Delta z)^3} (u_{i+2} - 2u_{i+1} + u_{i-1} - u_{i-2}) \quad (17)$$

$$u_i'''' = \frac{1}{(\Delta z)^4} (u_{i+2} - 4u_{i+1} + 6u_i - 4u_{i-1} + u_{i-2}) \quad (18)$$

Then, the general differential equations of the beam-column can be represented in an algebraic form by replacing the derivatives of the three equilibrium equations (Equation 14) at each of the pivoted points by the

appropriate central difference quantities (Equations 15- 18).

The following system of simultaneous algebraic equations is obtained:

$$u_{i-2} + a_1 u_{i-1} + a_2 u_i + a_3 u_{i+1} + u_{i+2} + b_1 \theta_{i-1} + b_2 \theta_i + b_3 \theta_{i+1} = C_x \quad (19\ a)$$

$$v_{i-2} + c_1 v_{i-1} + c_2 v_i + c_3 v_{i+1} + v_{i+2} + d_1 \theta_{i-1} + d_2 \theta_i + d_3 \theta_{i+1} = D_x \quad (19\ b)$$

$$\theta_{i-2} + g_1 \theta_{i-1} + g_2 \theta_i + g_3 \theta_{i+1} + \theta_{i+2} + e_1 u_{i-1} + e_2 u_i + e_3 u_{i+1} + f_1 v_{i-1} + f_2 v_i + f_3 v_{i+1} = P_x \quad (19\ c)$$

where:

$a_1 = \frac{P\,\Delta z^2}{EI_y} - 4$; $a_2 = 6 - \frac{2\,P\,\Delta z^2}{EI_y}$; $a_3 = \frac{P\,\Delta z^2}{EI_y} - 4$

$b_1 = -\frac{\{[P(e_y - \eta_o) + Q_y (z-L)z/2]\Delta z^2 - Q_y (z-L/2)\,\Delta z^3\}}{EI_y}$; $b_2 = -\frac{\{Q_y \Delta z^4 - 2[P(e_y - \eta_o) + Q_y (z-L)z/2]\Delta z^2\}}{EI_y}$

$b_3 = -\frac{\{[P(e_y - \eta_o) + Q_y (z-L)z/2]\Delta z^2 + Q_y (z-L/2)\,\Delta z^3\}}{EI_y}$

$C_x = \frac{\Delta z^4}{EI_y}\{Q_x + P[B_o \frac{z^2}{L^2} \sin\frac{\pi z}{L} - u_L''] - [P(e_y - \eta_o) + Q_y \frac{(z-L)z}{2}](D_o \frac{z^2}{L^2} \sin\frac{\pi z}{L} - \theta_L'') + Q_y (2z-L)(D_o \frac{z}{L}\cos\frac{\pi z}{L} + \theta_L') + Q_y (D_o \sin\frac{\pi z}{L} + \theta_L)\}$

$c_1 = \frac{P\,\Delta z^2}{EI_x} - 4$; $c_2 = 6 - \frac{2\,P\,\Delta z^2}{EI_x}$; $c_3 = \frac{P\,\Delta z^2}{EI_x} - 4$

$d_1 = \frac{\{[P(e_x - \xi_o) + Q_x (z-L)z/2]\Delta z^2 - Q_x (z-L/2)\,\Delta z^3\}}{EI_x}$; $d_2 = \frac{\{Q_x \Delta z^4 - 2[P(e_x - \xi_o) + Q_x (z-L)z/2]\Delta z^2\}}{EI_x}$

$d_3 = \frac{\{[P(e_x - \xi_o) + Q_x (z-L)z/2]\Delta z^2 + Q_x (z-L/2)\,\Delta z^3\}}{EI_x}$

$D_x = \frac{\Delta z^4}{EI_x}\{Q_y + P[C_o \frac{z^2}{L^2} \sin\frac{\pi z}{L} - v_L''] + [P(e_x - \xi_o) + Q_x \frac{(z-L)z}{2}](D_o \frac{z^2}{L^2} \sin\frac{\pi z}{L} - \theta_L'') - Q_x (2z-L)(D_o \frac{z}{L}\cos\frac{\pi z}{L} + \theta_L') - Q_x (D_o \sin\frac{\pi z}{L} + \theta_L)\}$

$g_1 = -\frac{\{[(z-L/2)(Q_x \xi_o + Q_y \eta_o)/2 - \overline{K'}/2]\,\Delta z^3 + (G K_T + \overline{K} + \overline{B})\,\Delta z^2\}}{EI_\omega} - 4$

$g_2 = 6 + \frac{\{2(G K_T + \overline{K} + \overline{B})\,\Delta z^2 + (Q_x \xi_o + Q_y \eta_o)\,\Delta z^4\}}{EI_\omega}$

$g_3 = \frac{\{[(z-L/2)(Q_x \xi_o + Q_y \eta_o)/2 - \overline{K'}/2]\,\Delta z^3 - (G K_T + \overline{K} + \overline{B})\,\Delta z^2\}}{EI_\omega} - 4$

$f_1 = \frac{\{[P(e_x - \xi_o) + Q_x (z-L)z/2]\Delta z^2\}}{EI_\omega}$; $f_2 = -\frac{\{2[P(e_x - \xi_o) + Q_x (z-L)z/2]\Delta z^2 + Q_x \Delta z^4\}}{EI_\omega}$

$f_3 = \frac{\{[P(e_x - \xi_o) + Q_x (z-L)z/2]\Delta z^2\}}{EI_\omega}$; $e_1 = -\frac{\{[P(e_y - \eta_o) + Q_y (z-L)z/2]\Delta z^2\}}{EI_\omega}$

$e_2 = \frac{\{2[P(e_y - \eta_o) + Q_y (z-L)z/2]\Delta z^2 + Q_y \Delta z^4\}}{EI_\omega}$; $e_3 = -\frac{\{[P(e_y - \eta_o) + Q_y (z-L)z/2]\Delta z^2\}}{EI_\omega}$

$P_x = \frac{\Delta z^4}{EI_\omega}\{\overline{K}[\theta_L'' - D_o \frac{z^2}{L^2}\sin\frac{\pi z}{L}] + Q_x \xi_o - Q_y \eta_o - \frac{2z-L}{2}(Q_x \xi_o + Q_y \eta_o)(\theta_L' + D_o \frac{z}{L}\cos\frac{\pi z}{L}) - (Q_x \xi_o + Q_y \eta_o)(\theta_L + D_o \sin\frac{\pi z}{L}) + [P(e_x - \xi_o) + Q_x \frac{(z-L)z}{2}](C_o \frac{z^2}{L^2}\sin\frac{\pi z}{L} - v_L'') - [P(e_y - \eta_o) + Q_y \frac{(z-L)z}{2}](B_o \frac{z^2}{L^2}\sin\frac{\pi z}{L} - u_L'') + Q_x (C_o \sin\frac{\pi z}{L} + v_L) - Q_x (B_o \sin\frac{\pi z}{L} + u_L)\}$

It is to recognize that the displacements u,v and θ are depending on cross section properties, the displacements of the Center of Gravity and the rotation of the principal axes. On the other hand, cross section properties and displacements are also depending on the occurred displacements. This means that a direct solution of this system of equations is not possible. For this reason , a combination of the finite difference method and the method of successive approximation is applied.

The method of successive approximation can be summarized in the following flow chart given in Figure 3.

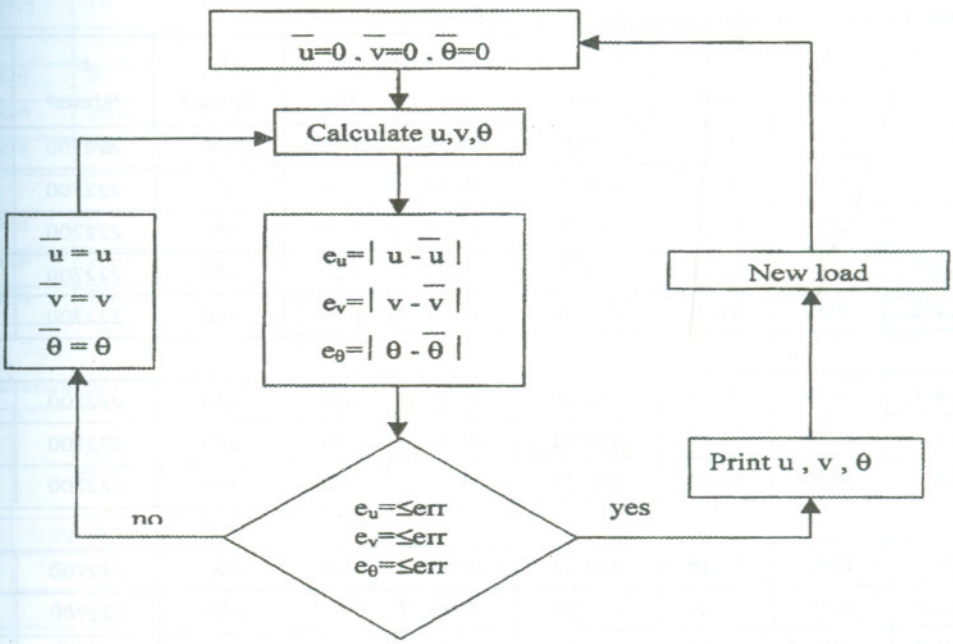

Figure 3 Flow chart for the method of successive approximation

Where u , v and θ are initial values for the unknown deformation , and (err) is a very small control value .

To enable the realization of this solution strategy , a computer program is developed (coded in FORTRAN 77) .

NUMERICAL MODEL VERIFICATION

In order to verify the simplicity, accuracy and efficiency of the proposed model for predicting the deformational response of columns, a number of experimental examples of Thomasson [7], Loughlan [8], Pekoz [9, 10], Fahmy [11] and Abo-Tabikh [12] have been selected, the ultimate load and deformations were calculated by using the numerical model. The initial imperfection [13] of L/500 for B_o,C_o and 1/300 rad for D_o was taken into consideration. The ultimate load was compared with the ultimate load calculated by both of Egyptian code and AISI.

Tables 1 and 2 present the dimensions of some numerical examples with C [11, 12] and Z [15] cross section. The typical sections are shown in Figure 4. Tables 3 and 4 and Figures 5 and 6 show true relation between p_{EX} and (P_{TH}, P_{AISI}, P_{EC}).

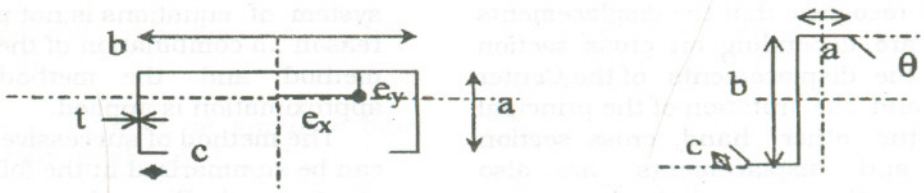

Figure 4 The Thin-Walled cross section examined theoretically or experimentally

Table 1 Cross Sectional Dimensions

CL	L mm	a mm	b mm	c mm	T Mm	F_y N/mm²	E N/mm²	E_x mm	E_y mm
CL1-1	3040	91.17	240.83	29.66	1.50	330	222700	0.00	0.00
CL1-2	3040	91.14	240.46	30.04	1.50	330	222700	0.00	-30.49
CL1-3	3040	91.11	240.76	29.67	1.50	330	222700	0.00	28.13
CL1-4	3040	91.04	240.52	29.72	1.50	330	222700	0.00	-61.88
CL1-5	3040	91.34	240.34	30.09	1.50	330	222700	0.00	0.00
CL2-1	3040	91.18	240.29	29.85	1.50	330	222700	60.00	14.06
CL2-2	3040	91.11	240.51	30.22	1.50	330	222700	60.00	-30.94
CL2-3	3040	91.11	240.43	30.77	1.50	330	222700	60.00	0.00
CL3-1	3040	91.18	240.21	30.05	1.50	330	222700	60.00	28.13
CL3-2	3040	91.17	240.24	30.41	1.50	330	222700	60.00	-61.88
CL3-3	3040	91.18	240.39	29.82	1.50	330	222700	100.00	0.00
CL4-1	3040	91.19	240.46	30.75	1.50	330	222700	100.00	-30.94
CL4-2	3040	91.23	240.40	29.94	1.50	330	222700	100.00	14.06
CL4-3	3040	91.04	240.36	29.85	1.50	330	222700	100.00	28.13
CL4-4	3040	91.17	240.00	30.00	1.50	330	222700	100.00	-61.88
CL5-1	2505	80.00	220.00	20.00	1.50	360	204100	0.00	0.00

Table 2 Cross sectional dimensions for Z shapes

CL	L mm	θ °	a mm	b mm	c mm	t mm	F_y N/mm²	E N/mm²	e_x mm	e_y mm
Z1	457.2	0	72.49	108.78	0	2.00	289	222700	0.00	0.00
Z2	457.2	29	50.95	100.89	15.37	2.01	289	222700	0.00	0.00
Z3	457.2	78	52.37	101.45	15.7	2.03	289	222700	0.00	0.00
Z4	914.4	0	73.71	101.37	0	2.06	392	222700	0.00	0.00
Z5	914.4	33	52.53	101.22	15.44	2.06	392	222700	0.00	0.00
Z6	914.4	78	52.07	101.32	15.60	2.06	392	222700	0.00	0.00
Z7	1524	0	74.04	101.47	0	2.06	420	222700	0.00	0.00
Z8	1524	33.1	52.25	101.47	15.72	2.03	420	222700	0.00	0.00
Z9	1524	78	52.53	101.24	15.52	2.03	420	222700	0.00	0.00
Z10	2438	0	73.76	101.75	0	1.93	289	222700	0.00	0.00
Z11	2438	31.1	52.22	100.35	15.49	1.96	289	222700	0.00	0.00
Z12	2438	80	51.99	101.70	15.04	1.93	289	222700	0.00	0.00

Table 3 Evaluation of C cross shapes results

CL	P_{TH} kN	P_{EX} kN	P_{TH} / P_{EX}	P_{AISI} kN	P_{TH} / P_{AISI}	P_{EC} kN	P_{TH} / P_{EC}
CL1-1	72.100	71.25	1.012	74.320	0.970	74.610	0.966
CL1-2	53.428	58.25	0.917	57.970	0.922	57.580	0.928
CL1-3	41.072	46.5	0.883	46.560	0.882	47.110	0.872
CL1-4	33.185	36.40	0.912	37.890	0.876	38.360	0.865
CL1-5	70.132	73.10	0.959	75.300	0.931	75.700	0.926
CL2-1	41.490	48.40	0.857	47.800	0.868	48.200	0.861
CL2-2	43.000	48.00	0.896	48.670	0.884	48.830	0.881
CL2-3	55.488	63.30	0.877	59.450	0.933	59.300	0.936
CL3-1	38.639	41.70	0.927	41.840	0.923	41.330	0.935
CL3-2	31.024	28.60	1.085	34.510	0.899	34.450	0.901
CL3-3	47.932	53.25	0.900	51.310	0.934	51.020	0.939
CL4-1	41.264	46.50	0.887	44.240	0.933	43.670	0.945
CL4-2	39.000	43.30	0.901	42.740	0.912	42.890	0.909
CL4-3	34.102	36.60	0.932	37.110	0.919	37.270	0.915
CL4-4	26.339	27.20	0.968	29.840	0.883	31.640	0.832
CL5-1	84.530	82.20	1.028	89.80	0.941	90.10	0.938

Table 4 Evaluation of Z Shapes Results

CL	P_{TH} kN	P_{EX} kN	P_{TH}/P_{EX}	P_{AISI} kN	P_{TH}/P_{AISI}	P_{EC} kN	P_{TH}/P_{EC}
Z1	74.556	84.551	0.882	88.996	0.838	85.936	0.868
Z2	110.068	99.326	1.108	109.254	1.007	108.793	1.012
Z3	137.536	142.441	0.966	143.226	0.960	140.577	0.978
Z4	94.176	106.83	0.882	105.948	0.889	103.201	0.913
Z5	135.182	129.100	1.047	123.116	1.098	126.059	1.072
Z6	162.061	164.612	0.985	165.554	0.979	160.197	1.012
Z7	83.091	88.996	0.934	89.86	0.925	87.211	0.953
Z8	118.946	115.218	1.032	107.272	1.109	109.578	1.085
Z9	141.264	129.041	1.095	132.18	1.069	134.299	1.052
Z10	49.050	44.498	1.102	50.031	0.980	51.404	0.954
Z11	68.376	59.596	1.147	57.604	1.187	67.895	1.007
Z12	71.417	66.747	1.070	65.433	1.091	69.847	1.022

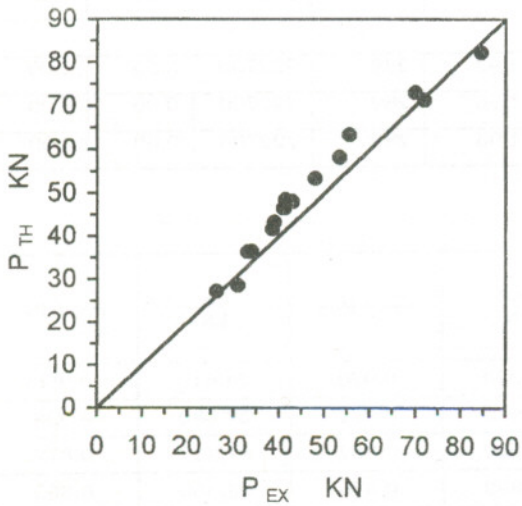

Figure 5 Relation between P_{EX} and P_{TH}

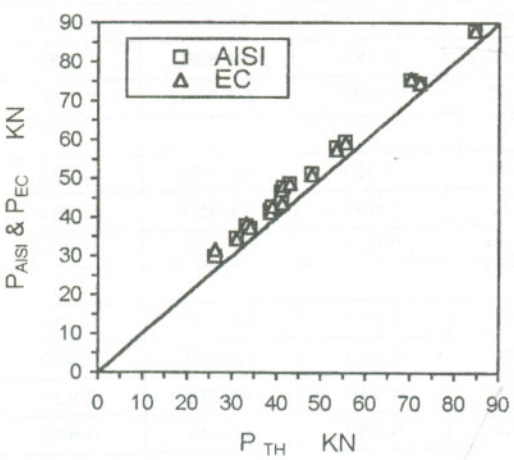

Figure 6 Relation between P_{TH} and Codes

Figure 4 presents the relation between P_{EX} and P_{TH}. It is obvious that the variation between the results obtained from the model and the results obtained experimentally not exceeds 12 %.

Figure 5 presents the relation between P_{TH} and (AISI, EC). It is obvious that the variation between the results obtained from the model and the results obtained experimentally not exceeds 16 %.

From the above mentioned comparative study, its clear that the efficiency of the present model is verified. It was found also that the model results are in good concordance with both AISI and Egyptian Code.

SYSTEMATIC APPLICATION

The results of the model presented in the previous comparative study encouraged the author to generate some applications. The results of these applications could be used in designing and manufacturing the thin-walled cross section .

Local buckling study for C section

In cold formed steel members [14], individual elements are usually so thin with respect to their width. These thin elements may be buckled locally, at stress level less than the yield point if, they are subjected to compression, shear, bending. Local buckling of individual elements of steel sections has been one of the major design criteria . It is well known that steel element will not fail when the critical local buckling stress F_{cr} ,

given by Equation 20 is reached. The element will continue to carry additional load by means of the redistribution of stress after local buckling occurs. The stress distribution is uniform until reaching the critical local buckling stress F_{cr} of the element. Then the element starts to buckle and the portion of the post buckling load of the center strip transfers to the edge portion of the element. This redistribution of stress continues until the stress at the edge of the element reaches the yield point of steel and then the elements begins to fail.

$$F_{cr} = K\frac{\pi^2 E}{12(1-\mu^2)}\frac{t^2.}{w^2} \qquad (20)$$

where
w the length of the element
t the thickness of the element
K= 4 for interior element (stiffened element) and 0.425 for outer element (unstiffened element)

The ratio between the length (w) and the thickness (t) for the individual element controls the local buckling, the limit value for this ratio was studied for both columns with C cross section of steel 52 as shown in Figure 7.

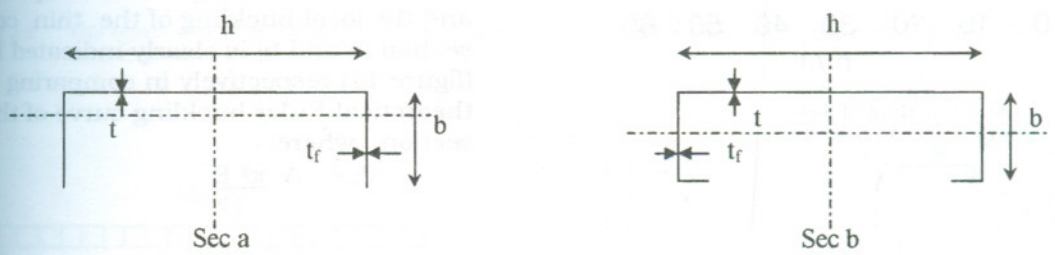

Figure 7 Thin Walled C cross-section

From Figure 8, the lib prevents local buckling in the range of:

$$11 \le b / t_f < 20.5 \text{ or } \frac{20.87}{\sqrt{F_y}} b/t_f < \frac{38.90}{\sqrt{F_y}}$$

and from Figure 9, it is obvious that the web has local buckling when :

$$h/t \ge 30 \text{ or } h/t \ge \frac{56.921}{\sqrt{F_y}}$$

Table 5 shows the comparison of these limits with the Egyptian code and the American code for steel 52.

Table 5: Limits of h/t

Case	Model	American code	Egyptian code	Euro code
Stiffened element	$\frac{56.921}{\sqrt{F_y}}$	$\frac{58.63}{\sqrt{F_y}}$	$\frac{45.000}{\sqrt{F_y}}$	$\frac{58.63}{\sqrt{F_y}}$
Unstiffened element	$\frac{20.870}{\sqrt{F_y}}$	$\frac{56.921}{\sqrt{F_y}}$	$\frac{56.921}{\sqrt{F_y}}$	$\frac{56.921}{\sqrt{F_y}}$

It was found that the model is in good agreement with the American code and the Euro code; the difference is less than 8%, but the difference in comparing with the Egyptian code limits is about 20%.

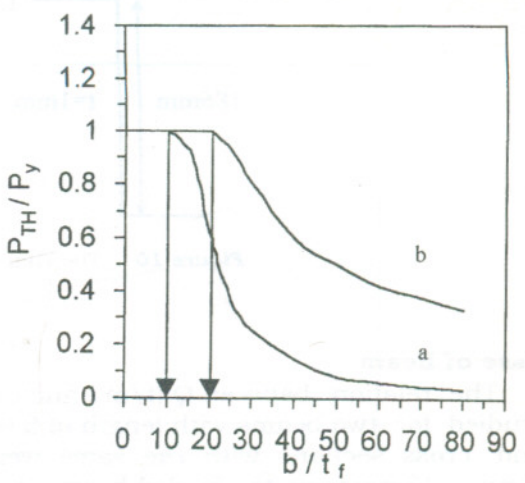

Figure 8 Local Buckling of flange

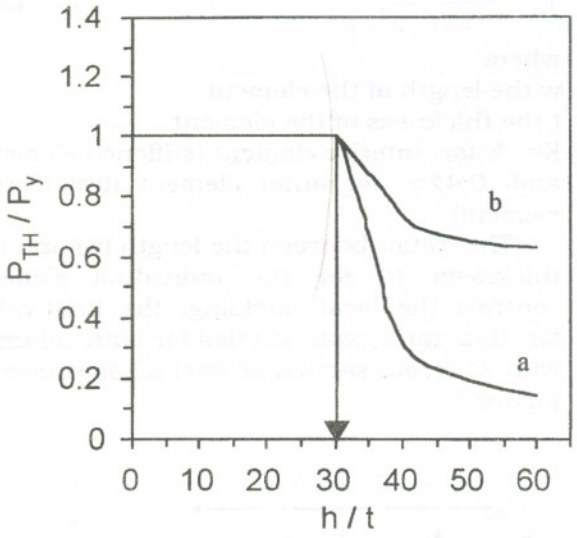

Figure 9 Local buckling of web

Case of Column

The relation between P and δ was studied for three columns with length of 2.00 m and different cross sections shown in Figure 10, these three columns have the same weight. The relation between P and λ was studied for sections a and b , and the results are plotted in Figure 11.

From Figure 12, the column of (section a) has low ultimate resistance with big deflection , while the column with (section c) presents the best behavior (ultimate resistance and deflection) in comparing with the other sections .

The effect of the geometric imperfection and the local buckling of the thin column section (a and b) is clearly indicated in (figure 11) respectively in comparing with the theoretical Euler buckling curve of the same section , where:

$$P_E = A \frac{\pi^2 E}{\lambda^2}$$

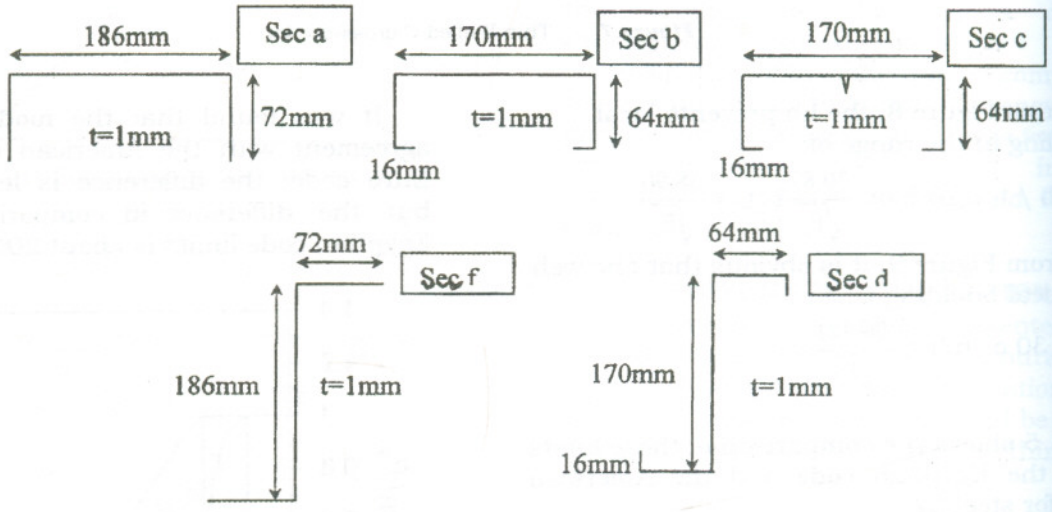

Figure 10 The Thin-Walled cross sections used in applications

Case of Beam

The relation between Q (t/m`) and δ was studied for two beams with length of 6.00 m and cross sections with the same weight. Figure 13 presents the loaded beam and the studied cross sections .

The effect of the lib could be easily noted from Figure 14, where the beam of the cross section (b) presents a relatively good behavior in comparing with the beam of the cross section (a).

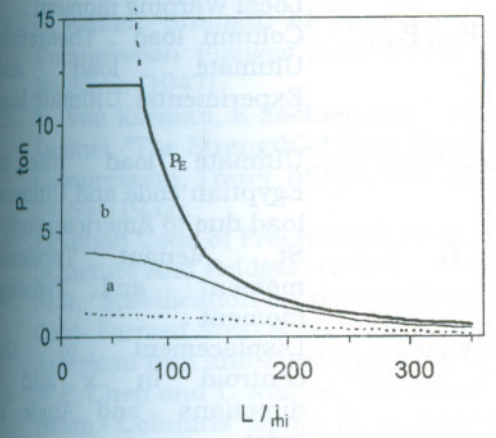

Figure 11 The relation between P and λ for a column with C cross-section

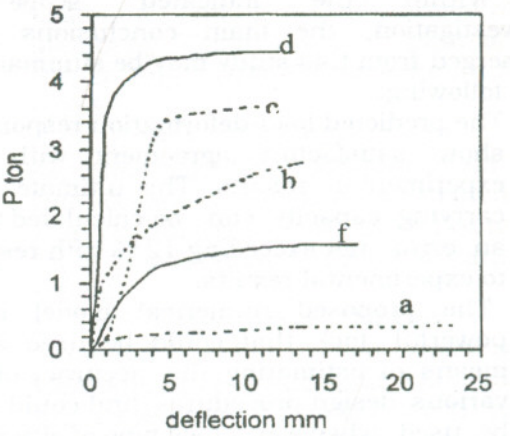

Figure 12 relation between P and δ for a column with C cross section

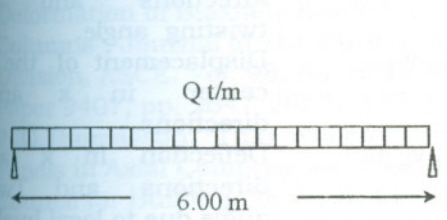

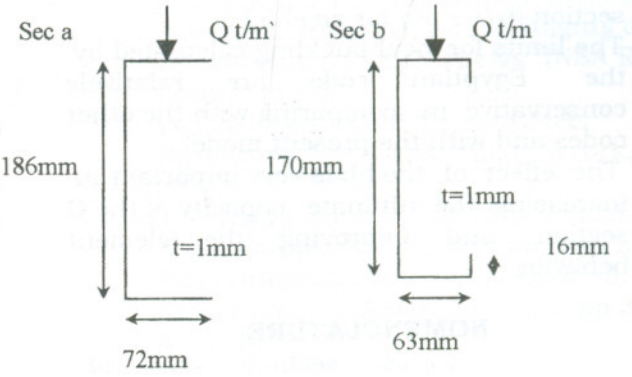

Figure 13 He beam loaded by uniform load Q t/m`

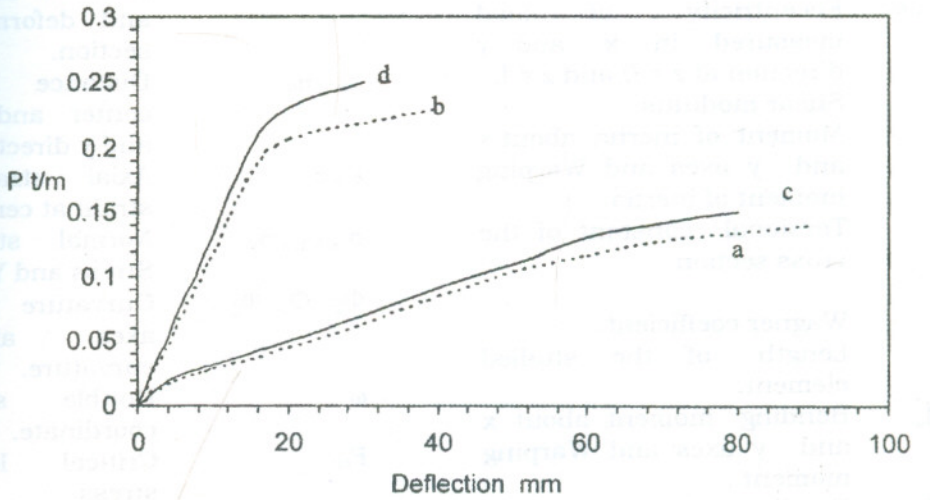

Figure 14 Relation between P (t/m) and δ for a beam with C cross-section

CONCLUSION

Within the indicated scope of investigation, the main conclusions that emerged from this study may be summarized as following:

1. The predicted load-deformation responses show satisfactory agreement with the experimental results. The ultimate load carrying capacity can be calculated with an error not exceeding 12 % with respect to experimental results.
2. The proposed numerical model is a powerful tool that could be used as a means of estimating the accuracy of the various design procedures, and could also be used whenever a new type of situation not covered by simplified methods is encountered.
3. The load decrease with (h/t) of the cross section ($h/t \geq 30$) for steel 52 .
4. The limits for local buckling calculated by the Egyptian code are relatively conservative in comparing with the other codes and with the present model .
5. The effect of the lib is very important in increasing the ultimate capacity of the C section and improving the element behavior.

NOMENCLATURE

A	Cross section area of element section.
B_o , C_o , D_o	Initial Imperfection in x,y direction and twist .
E	Young's modulus.
e_{xo} , e_{yo} , e_{xl} , e_{yl}	Eccentricity of load measured in x and y direction at z = 0 and z = L.
G	Shear modulus.
I_x , I_y , I_ω	Moment of inertia about x and y axes and Warping moment of inertia.
K_T	Torsional constant of the cross section.
$\overline{K}$	Wagner coefficient.
L	Length of the studied element.
M_x , M_y , M_ω	Bending moment about x and y axes and Warping moment .
M_ξ , M_η , M_ζ	Bending moment about local axes ξ and η and Local Warping moment .
P, P_{th} , P_{ex} ,	Column load , Theoretical Ultimate load and Experimental Ultimate load .
P_{EC} , P_{AISI}	Ultimate load due to Egyptian code and Ultimate load due to American code
T_{sv} , T_w	St.. Venant Torsional moment and Twisting moment .
u , v , θ	Displacement of the centroid in x and y directions and Angle of twist .
u_o , v_o , θ_o	Initial deflection of the centroid in x and y directions and Initial twisting angle.
u_m , v_m	Displacement of the shear center in x and y directions.
u_L , v_L , θ_L	Deflection in x and y directions and Twisting angle due to local buckling.
x , y , z	Local coordinate system whose origin moves with the cross section and whose axes are always parallel to X,Y,Z axes.
X , Y , Z	Global coordinate system fixed in space .
ξ , η , ζ	Local coordinate system fixed to the cross section and deforming with cross section.
ξ_o , η_o	Distance between shear center and centroid in x and y directions.
ε , ε_o	Axial strain and Axial strain at centroid.
σ , σ_r , σ_y	Normal stress, Residual Stress and Yield stress.
Φ_ξ , Φ_η , Φ_ζ	Curvature about ξ and η axes and Warping curvature.
ω	Double sectorial area coordinate.
F_{cr}	Critical local buckling stress.
λ	Effective slenderness ratio.

REFERENCES

1. G. Winter, "Strength of Thin Steel Compression Flanges", Cornell Bulletin No.35/3, (1947)
2. T. Von Karman, E Sechler and L.H. Donnel, "The Strength of Thin Plates in Compression, Trans. ASME, Vol. 54, pp. 54-55, (1932).
3. Egyptian Code of Practices of Steel Structure And Bridges, (1989).
4. AISI, "Specification for the Design of Cold- Formed Steel Structural Members", American Iron and Steel Institute, (1980)
5. W.F. Chen and T. Atsuta, "Theory of Beam - Columns" Space Behavior and Design", Vol.2, Mc Graw Hill, New York, (1977).
6. L. A. Soltis and P. Christiono, "Finite Deformation of Biaxially Loaded Columns", Journal of The Structural Division, ASCE. Vol. 98, No. ST12. Proc. Paper 9407, pp. 2647-2662, (1972).
7. P. O.Thomasson, "Thin-Walled C-Shaped Panels in Axial Compression", Swedish Council for Building Reseach, d1, (1978).
8. J. Loughlan, "Mode Interaction in Lipped Channel Column Under Concentric or Eccentric loading", Ph.D. Thesis, University of Strathclyde, Glasgow, (1979).
9. T. Pekoz, and T. Loh, "Combined Axial Load and Bending in Cold-Formed Steel Members", M. S. Thesis, Cornell University, New York, (1982).
10. T. Pekoz, and T. Loh, "Combined Axial Load and Bending in Cold-Formed Steel Members", Report No. 85-3, Dept. of Struct. Eng., Cornell University, N.Y., (1985).
11. A. S. Fahmy, "Theoretische and experimentelle Untersuchungen zur Interaktion von Knicken und Beulen bei Dunnwandigen Kaltgeformten Bauteilen", Ph.D. Dissertation, Universitat Karlsruhe, (1988)
12. R. Ahmed Abo-Tabikh, "Flexural-Torsional Buckling of Cold-formed Steel Columns under Axial Load: Theoretical and Experimental Studies", Ph.D. Thesis, Faculty of Eng., University of Alexandria, (1994).
13. Abdel Aziz Mahmoud, "Model Numerique pour l' Etude du Flambement des Poteaux Soumis al' Incendie avec Gradignts de Temperature ", Ph.D. Thesis "INSA Renne-France. (1987).
14. Yu, Wei-wen, "Cold-Formed Steel Structures", Mc Graw Hill, NewYork, (1973).
15. D. Polyzois, and A. R. Sudharmapal, "Cold Formed Steel Z-Section with Sloping Edge Stiffness Under Axial Load". J. Struct. Engrg., ASCE, Vol. 116, pp.392-406, (1990).

Received December 30, 1998
Accepted February 18,1999

محاكاة لسلوك الاعمده ذات الجدران الرقيقة والقطاعات الغير متماثلة

عبد العزيز محمود ابراهيم* ، أحمد رأفت أبو طبيخ* و أحمد نور الدين**

* قسم الهندسة الأنشائية - جامعة الاسكندرية

** المجموعة العربية للإنشاءات

ملخص البحث

فى هذا البحث، تم اعداد نموذج رياضى ليمثل سلوك الكمرات والاعمدة ذات الرفيعة تمثيلا دقيقا حتى الوصول الى الحمل الاقصى. وقد أخذ فى الاعتبار لامركزية الاحمال وشروط الحافة المتوقعة . كذلك حالة القطاع من حيث كونه متماثل او غير متماثل وتعرض بعض الاجزاء منه الى ترخيم اثناء التحميل القطاع و كذلك تغير الجساءة الانحنائية والالتوائة للقطاع. وحتى يكون النموذج النظرى اقرب ما يمكن للعمود الحقيقى فقد تم اخذ الاعوجاج الابتدائى (**Initial deformations**) فى الإعتبار. ولقد استخدمت طريقة الفروق المحدودة (**Finite Difference**) فى الاتجاه الطولى للعمود او الكمرة لتحويل المعادلات التفاضلية التى تحكم سلوك العنصر تحت تأثير الاحمال المختلفة الى معادلات جبرية.

وبناء على ماسبق فقد تم كتابة برنامج للحاسب الالى باستخدام لغة الفرتران ومقارنة النتائج المتاحة للتاكد من دقة البرنامج ثم اجرينا مقارنة بين نتائج البرنامج والنتائج المحسوبة كل من المواصفات الامريكية والمصرية . كذلك تم دراسة العديد من النتائج واستنتاج بعض العلاقات ومقارنتها بالمواصفات.